The Analyst

Association of desferrioxamine with humic substances and their interaction with cadmium(II) as studied by pyrolysis–gas chromatography–mass spectrometry and nuclear magnetic resonance spectroscopy†

Richard. M. Higashi*[a], Teresa. W-M. Fan[b] and Andrew N. Lane[c]

[a] *Crocker Nuclear Laboratory, University of California, Davis, CA 95616, USA*
[b] *Department of Land, Air and Water Resources, University of California, Davis, CA 95616, USA*
[c] *Division of Molecular Structure, National Institute for Medical Research, Mill Hill, UK NW7 1AA*

In soils, sediments and aqueous media, the existence of any significant association of organic ligands with humic substances (HS) would complicate metal ion equilibria and kinetics beyond those of existing models that assume competition among non-interacting ligands. Multi-dimensional NMR techniques were applied to obtain kinetic and structural evidence of extensive association of desferrioxamine B (DFOB) with HS. This occurred through diaminopentyl and succinyl protons of DFOB with the aromatic/phenolic and/or saccharidic groups of HS, and exhibited an exchange rate of 15 000–25 000 s^{-1}. Additionally, the aqueous interaction of HS, DFOB and Cd^{II} was probed using pyrolysis–GC–MS analysis directly of microliter volumes. Although pyrolysis–GC–MS data can be difficult to interpret alone, the NMR characterization of ligand–HS association enabled the results to be interpreted. Pyrolysis–GC–MS revealed thermolyzate markers that permitted the quantification of total DFOB and apparent complexes of DFOB·Cd and HS·Cd. The results indicate that the formation of DFOB·HS (or possibly DFOB·Cd·HS) caused significant decreases in the formation of the chelator complex, DFOB·Cd. This decrease did not fit with equilibrium-based concepts since the order of addition strongly influenced all results. Although previously unknown, the results show that such organic ligand–HS interactions do occur, which significantly alter the metal ion chemistry and probably affect bioavailability; the latter is relevant since DFOB is a siderophore synthesized by bacteria to acquire metal ions. Therefore, in order to understand the bioavailability of metal ions in real systems such as the rhizosphere one must consider the interactions of HS with biogenic ligands, for which liquid-state multi-dimensional NMR is a powerful tool. Unlike metal–ligand measurements that are limited to liquid state and/or low paramagnetic samples, the pyrolysis–GC–MS method has the potential to be extended to whole soils and sediments for the analysis of metal ion speciation.

Keywords: *Siderophore; humic substances metal ions; exchange kinetics; biogenic ligands; bioavailability*

Organic matter in the environment regulates the fate of metal ion pollutants by sorption, which in turn can have major effects on the transport and bioavailability of metal ions. However, the mechanisms by which mobile, low molecular mass organic ligands affect the sorption of cationic metal ions is poorly understood in natural systems such as soil and sediment, since they consist of a vast array of mobile and immobile (macromolecular) ligands.

The mobile organic ligands can have K_d values for metal ions that span more than eight orders of magnitude, depending on the chemical structure.[1] Some of the most powerful ligands known are not limited to the laboratory and are actually found in the environment, such as bacterial and plant siderophores. The exudation of such compounds by plants and bacteria is the principal mechanism through which they acquire metal ions. Since the bioavailability of metal ions is a central concern in human health, ecotoxicology, plant and microbial nutrition and bioremediation, studies involving these biogenic ligands are badly needed. Fortunately, the long-standing analytical barriers to the comprehensive study of complex mixtures of biogenic ligands are now being overcome, by using multi-dimensional NMR and GC–MS to analyze directly unfractionated plant root exudates.[2]

In addition to the mobile organic ligands, soils contain a heterogeneous organic component that consists of macromolecular colloidal particles in association with the mineral matrix. These so-called humic substances (HS) are relatively non-diffusable, and can therefore be considered as immobile in this context. HS is considered to be a powerful metal ion binding agent,[3] but is structurally undefined, as it is the product of reactions with a broad spectrum of natural substances.[4] Hence HS genuinely rank among the most complex and least-understood natural substances known , and have been described by such contradictory terms as ‘polymeric’ and ‘amorphous’. Despite the complexity of HS, recent work appears to be leading to good predictability of metal ion binding in isolated metal–HS systems, accomplished using a wide range of techniques.[5–10] It is also clear that a study of the relevant structural features of HS is crucial to understanding the mechanisms of metal binding,[6,11,12] but studies addressing this aspect are rare.

For the few studies involving both mobile and immobile ligands, the prevailing mechanistic view of metal ion binding is that of competition among ligand sites,[13] and are uniformly based on simple organic acids. In more complex experiments, metal ion binding into organic ligand–metal–HS associations appear to be weak in comparison with a system containing only low molecular mass ligands.[14]

Unfortunately, these studies do not account for the conditions that exist in very active metal-uptake environments such as the rhizosphere, which is needed for understanding bioavailability, its potential ecotoxic effects and efficacy for bioremediation and nutrition. There, organic ligands consist of simple acids, unusually powerful ones such as siderophores, and extremely complex ones such as HS, all at concentrations far higher than in the bulk soil. In such systems, a powerful soluble organic

† Presented at The Third International Symposium on Speciation of Elements in Toxicology and in Environmental and Biological Sciences, Port Douglas, Australia, September 15–19, 1997.

ligand, the bacterial siderophore desferrioxamine B (DFOB), was postulated to be sorbed by organic matter on whole soil,[15] and indirect evidence was presented for its interaction with HS that was pre-saturated with Cu^{II} ion.[16]

The existence of any significant ligand–HS association, independent of the metal ion, would greatly complicate the situation beyond that of current complexation theory (*e.g.* ref. 17) and existing speciation models such as MINTEQA2.[13] Such models explicitly assume that all competing ligands act independently, *i.e.*, do not form complexes with one another that alter their binding properties. Thus, with the exception of ligand or ion removal via precipitation, cooperative or anti-cooperative effects are not included. In this paper, we provide kinetic and structural NMR evidence that DFOB associates extensively with HS in the absence of added metal ions. However, the analytical power of NMR is optimal at high analyte concentrations that may cause precipitation of HS by Cd^{II} We therefore probed some of the consequences of the HS–DFOB interaction by pyrolysis-GC–MS analysis directly of microliter volumes obtained from aqueous interaction experiments on HS, DFOB and Cd^{II}. The method yielded markers of total DFOB and apparent complexes of DFOB·Cd and HS·Cd. The sensitivity of the method allowed us to conduct experiments at lower concentrations that avoid precipitation of HS by Cd^{II}, while consuming only very small amounts of the limited–availability HS. Although pyrolysis–GC–MS evidence is often difficult to interpret alone, the NMR studies helped validate its use in obtaining unexpected and potentially significant trends of DFOB–HS–Cd interaction.

Experimental

Materials

Humic substances were isolated from freeze-dried soil from the Sierra Nevada mountains (CA, USA) ('Forbes' HS) and rice field soil obtained from Chikugo Prefecture, Japan ('Chikugo' HS) (a gift from Dupont Agricultural Products, Wilmington, DE, USA); the latter soil has a comprehensive record of crop conditions and applied chemicals. HS was extracted following the initial steps of Olk *et al.*[18] Briefly, 0.25 M NaOH was used for extraction at 10 °C with a helium purge, followed by centrifugation and then filtration of the supernatant; the filtrate HS was then precipitated by adjusting the pH to 2 using 0.2 M HCl, recentrifuged and the pellets were rinsed thoroughly in 0.01 M HCl before lyophilization. The lyophilized pellet was then extracted using 0.15 M 4,5-dihydroxybenzene-1,3-disulfonate (Tiron, Sigma, St. Louis, MO, USA) at pH 6.1 and 35 °C and the HS were precipitated by adjusting the pH to 2 using 0.2 M HCl, centrifuged, rinsed thoroughly in 0.01 M HCl and finally lyophilized. The Tiron treatment was repeated once, and the final HS pellet was dissolved in water and titrated to pH 6 with NaOH before lyophilization. Tiron exhaustively removed metal ions from HS,[19] allowing good quality NMR spectra to be acquired. Of greater importance, hydrolytic conditions were avoided, and Tiron does not bind to HS as other chelators (*e.g.*, EDTA) do, which substantially improves the relevance of the prepared HS for metal-binding and other studies.

Cadmium(II) was used in experiments in the form of $CdSO_4$ (Sigma) and desferrioxamine B methanesulfonate salt (DFOB) (a gift from Ciba-Geigy, Summit, NJ, USA) was used as received. According to ^1H and ^{13}C NMR spectroscopy, the DFOB did not contain significant organic contaminants. For the NMR experiments, Tiron-treated HS was adjusted to pH 7, lyophilized, dissolved in D_2O, and centrifuged for 5 min to remove particulates. The pD^* (apparent pD as measured using a pH electrode) of the final HS solution ranged from 5.5 to 6.2. For DFOB titrations of HS, 0.1 M DFOB in D_2O at pD^* 7.2 was prepared. For pyrolysis–GC–MS measurements, all experiments were performed at 25 °C and consisted of at least two of the three components (Cd, DFOB or Chikugo HS), each adjusted to pH 6.5 with HCl or NaOH, which were vortexed mixed in a polypropylene micro-centrifuge tube for 10 s and allowed to stand for 4 h before analysis. In three-component experiments, the third component was mixed in after 4 h, then allowed to stand for another 4 h before analysis. Each sample was run in a 100 μl total volume. There was no apparent stratification or separation of the solutions upon standing.

NMR analysis

All NMR spectra were recorded at 298 K on a Varian (Palo Alto, CA, USA) UnityPlus NMR spectrometer operating at 11.75 T or a Bruker (Karlsruhe, Germany) AM-400 spectrometer operating at 9.4 T. The one-dimensional (1-D) ^1H spectra of the Chikugo HS were acquired at 11.75 T with a 90° pulse, 5500 Hz spectral width, 1.6 s sampling time, 2 s relaxation delay and 128 transients, while those of the Forbes HS were obtained at 9.4 T with a 90¡ pulse, 4505 Hz spectral width, 1 s sampling time, 2 s relaxation delay, and 128 transients. The two-dimensional (2-D) ^1H total correlation NMR spectroscopy (TOCSY) of both Chikugo and Forbes HS was performed at 11.75 T with a 5000 Hz spectral width, 0.41 s and 51.2 ms sampling times in t_2 and t_1, respectively, a 2 s interpulse delay, a 46.1 ms isotropic mixing time with a 8.4 kHz spin-lock (B_1) field strength, 256 increments and 32 transients per increment,. The 2-D ^1H nuclear Overhauser effect NMR spectroscopy (NOESY) of Chikugo HS was carried out at 11.75 T using a 0.1–0.3 s mixing time, 5500 Hz spectral width, 0.372 s sampling time in t_2 and 23.2 ms in t_1, 2 s relaxation delay, 128 increments and 64 transients per increment. The NOESY spectrum of Forbes HS was acquired at 9.4 T using the parameters described in Fig. 1 (0.1 s mixing time, 4500 Hz spectral width, 2 s spectral width, 0.23 s sampling time in t_2 and 28.2 ms in t_1, 128 increments and 128–192 transients per increment). The spin–lattice relaxation time in the rotating frame, 1-D $T_{1\rho}$, was measured at 11.75 T using a 1 s sampling time, 2 s relaxation delay, 1.962, 3.924, and 8.4338 kHz, spin-lock field strengths 5.5–7 kHz spectral width, and spin-lock times of 7.7, 15.4, 34.6, 46, 65.3, 96, 146 ms. The $T_{1\rho}$ was calculated from fitting an exponential decay curve to the peak intensity I, versus spin-lock times τ according to

$$I(\tau) = I_0\exp(-\tau/T_{1\rho}) \quad (1)$$

where $I(\tau)$ is the peak intensity at spin-lock duration τ and I_0 is the intensity at $\tau = 0$.

Pyrolysis–GC–MS analysis

For pyrolysis–GC–MS analysis, 2–4 μl of sample were pipetted on to quartz wool in a quartz sample tube and the tube was placed in an analytical pyrolysis system (Pyroprobe 2000/AS2500, CDS, Oxford, PA, USA) interfaced to a Hewlett-Packard (Palo Alto, CA, USA) Model 5890 GC–5971A MS system equipped with a non-polar column (50 m × 0.15 mm, BPX-5 5% phenyl–methyl silphenylene siloxane copolymer, SGE, Austin, TX, USA). The quartz sample tube dropped by gravity into the pyrolysis chamber, followed by a 3 s delay to purge out residual air, then the pyrolysis carrier gas path was switched to on-line with the GC–MS system, the pyrolysis probe was heated at 800 °C for 10 s and volatile thermolyzates were swept by a helium stream into the GC column for 1 min, after which the pyrolysis system was switched off-line for thermal cleaning at a 20 ml min^{-1} helium flow for the duration of the analysis. The remainder of the analysis was conventional, with the thermolyzates eluting sequentially into the mass spectrometer for detection. The pyrolysis injector block was at 280 °C, the GC injector at 280 °C, the helium carrier gas velocity was kept constant at 40 cm s^{-1}, the injector split was

1 : 10, the column was temperature programmed from 40 °C (4 min hold) to 290 °C at 10 °C min^{-1} and the GC–MS interface was at 300 °C. The mass spectrometer conditions were electron ionization mode, 70 eV electron energy, source/manifold temperature 180 °C, electron multiplier voltage 1458 V, acquisition from *m/z* 40 to 400, three spectra averaged into one to yield one spectrum per second and centroid processing of data to yield the mass histograms, and the system was calibrated with respect to perfluorotributylamine using the Autotune function of the software.

Results and discussion

NMR evidence for the association of DFOB and HS

Without a demetallation step in the preparation of HS, the NMR spectra were of low quality, and little useful information could be obtained from 2-D experiments. However, after extensive Tiron treatment, the NMR spectral quality of HS improved such that useful information from 1-D and 2-D NMR experiments (*e.g.*, ^{1}H TOCSY and NOESY) was readily obtained. Fig. 1 illustrates the use of NMR for detecting interactions between DFOB with HS. The 1-D spectrum of DFOB shows a series of sharp resonances as expected for a relatively small, flexible molecule [Fig. 1(A)]. In the presence of HS, the resonances broaden [Fig. 1(B)] even though the DFOB is in large excess. Fig. 1(C) illustrates the corresponding 2-D NOESY contour plot of Forbes HS with excess DFOB, where the off-diagonal cross peaks were traced by rectangular boxes. The presence of these cross peaks indicate intra- and intermolecular interactions *via* exchange and dipolar interactions of functional groups represented by the diagonal peaks.

At least three lines of evidence for the association of DFOB with HS were obtained by NMR. First, the 1-D spectrum of HS with excess DFOB [Fig. 1(B)] had similar resonances to that of DFOB alone [Fig. 1(A)] except that the lines were significantly broadened in the mixture. This broadening effect indicated an exchange between HS and DFOB and, therefore, binding of DFOB to the HS macromolecule.

Second, in a titration of HS with DFOB, the positions of peaks arising from DFOB changed with increasing concentration (data not shown), which is characteristic of a fast exchange process on the chemical shift time-scale. Extrapolating from free DFOB to low concentration indicated a difference in chemical shifts of at least 80 Hz (0.16 ppm at 500 MHz) between the free and bound states. Hence the exchange rate constant must be at least 80π, which gives a dissociation rate constant $k_{exchange} \gg 250\ s^{-1}$. Unfortunately, as the concentration (or even the identity) of the interaction sites in the HS is unknown at this time, a dissociation constant could not be determined from these data. As the ligand and HS are in fast intermediate exchange, the line broadening can also be used to estimate the exchange rate constant using rotating frame relaxation.[20] Preliminary $T_{1\rho}$ measurements at 2, 4 and 8 kHz B_1 field strength (data not shown) yielded an exchange rate constant (equal to the sum of the dissociation rate constant and the apparent association rate constant) of 15 000–25 000 s^{-1}, verifying the fast exchange and indicating weak binding between HS and DFOB. The fast exchange also implies that a significant proportion of the DFOB molecules present was in exchange with HS. However, these data did not rule out the presence of sub-populations of DFOB with slower exchange and therefore stronger binding, as could be the case with a complex substance such as HS.

The third line of evidence of extensive DFOB association with HS comes from the NOESY spectrum [Fig. 1(C)], which provided the chemical nature of the interaction between HS and DFOB. In this type of spectroscopy, both dipolar (through-space) and exchange interactions among different proton-bearing functional groups of HS and DFOB are represented by the off-diagonal cross-peaks. A number of cross-peaks were those due to intramolecular interactions within HS and DFOB [a few examples are linked by thin solid and dashed lines in Fig. 1(C)]. However, there were new cross-peaks which arose when the two were mixed together [cross-peaks linked by thick gray lines in Fig. 1(C)], so they were not part of the HS or DFOB molecular network, and therefore must have been derived from the HS·DFOB complex. Furthermore, based on their chemical shifts, it appears that HS–DFOB interactions occurred through the diaminopentyl and succinyl protons of DFOB (assignments as per Borgias *et al.*[21]) with the aromatic/phenolic and/or saccharidic groups of HS.

Finally, very similar results along all three lines of NMR evidence were also obtained for the Chikugo HS (data not shown), suggesting that extensive DFOB and possibly other organic ligand association with HS may be a common phenomenon.

Therefore, unlike the previous report showing indirectly that HS pre-saturated with Cu^{II} ions may bind DFOB[16], Fig. 1 directly demonstrates that DFOB binds to HS even in the absence of any added metal ions. Because metal ions are expected to affect the properties of both HS and DFOB, the interactions among these components may also differ from those in the absence of added divalent cations. The effects of transition metal and DFOB titrations of HS on complex formation were the next to be studied. Unfortunately, the information-rich NMR could not be used because of HS precipitation in the presence of Cd^{II} at the concentrations required for NMR. Other, more common techniques (*e.g.*, UV–visible or infrared spectrophotometry) suffered from severe interference from HS and hence were not useful in practice. We therefore turned to pyrolysis–GC–MS, initially with the intent to obtain HS structural information in Cd^{II} addition experiments.

Pyrolysis–GC–MS analytical markers of DFOB, HS, and Cd^{II} interactions

Three analytical markers in pyrolysis–GC–MS were encountered en route to studying structural changes in Chikugo HS under Cd^{II} and DFOB treatment. These markers appeared to be separately quantitative for total DFOB and complexes of DFOB·Cd and HS·Cd. Furthermore, because the method is far more sensitive than NMR, it allowed us to conduct experiments at lower concentrations that avoid precipitation of HS and on a small scale (typically < 500 μg of HS in 100 μl), conserving laborious-to-isolate HS material.

The simultaneous analysis for these three markers is illustrated in Fig. 2, which shows the pyrolysis–GC–MS analysis of an aqueous mixture of DFOB, HS, and Cd^{II}. Although there were other peaks in the selected ion chromatograms in Fig. 2, as well as in other selected ion chromatograms, that responded to the desired analytes, those indicated in Fig. 2 were observed to be among the most reliable.

Total [DFOB] marker

Fig. 3(A) shows the molar response of the *m/z* 113 peak (see Fig. 2) to [DFOB]. A search of the NIH–NIST–EPA mass spectral library provided an excellent match of this peak with *N*-butylpyrrolidinedione (search results not shown), possibly formed through cyclization of a DFOB thermolyzate. This product was not seen among thermolyzates of HS. The data points plotted are a compilation from several experiments at various concentrations of Cd^{II} (0–100 mM) and HS (0–5

μg μl^{-1}) and pH values 4–8. Despite these variable conditions, the regression line has $r^2 > 0.99$. Hence, the DFOB analytical marker is independent of the other two constituents (see also black triangle plot, Fig. 4) and insensitive to conditions such as pH, possibly because it is a low-yield (unfavorable) thermolysis product of DFOB (data not shown), and hence insensitive to the formation conditions. Since the low yield is compensated for by the high sensitivity and selectivity of GC–MS, it shows promise for the microanalysis of total [DFOB] and other hydroxamate structures in more complex matrices such as soils and sediments.

[DFOB·Cd] marker

Fig. 3(B) shows the molar response of the *m/z* 140 peak (see Fig. 2) to various amounts of Cd^{II} added to 25 mM DFOB at pH 6.5; three replicate analyses are plotted to illustrate the raw variance. The regression line through the first five mixtures has $r^2 > 0.99$,

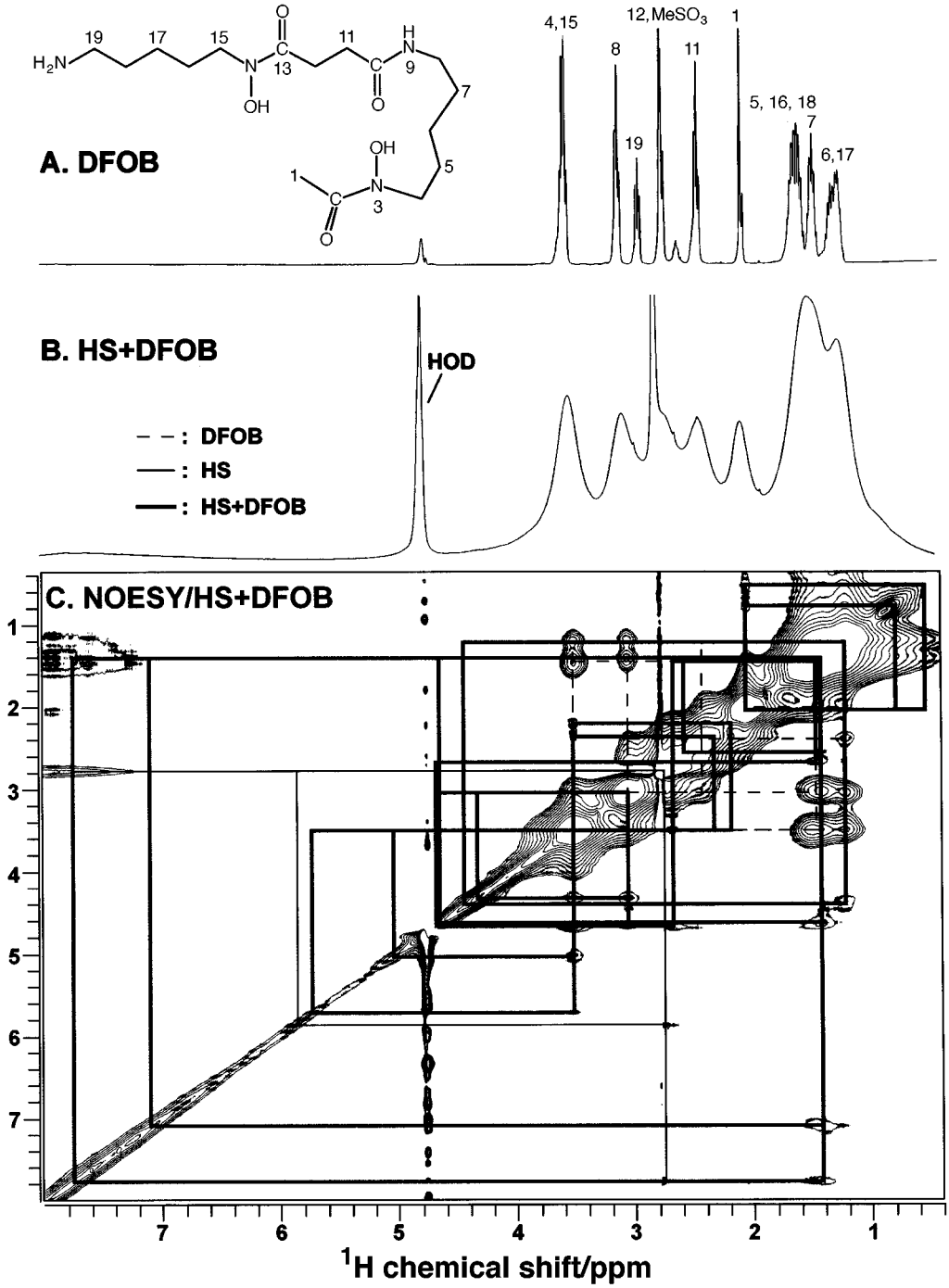

Fig. 1 NMR evidence for the interaction between DFOB and Forbes HS. A, Structure and ^{1}H NMR spectrum of desferrioxamine B (DFOB), a common and powerful organic ligand for transition metals in soils. Spectral assignments based on Borgias *et al.*[21] are numbered, and the spectrum is plotted with expanded ordinate to show detail, such that the peak labeled 12,$MeSO_3$ is cut off at the top. B, ^{1}H NMR spectrum of a humic substance (HS) at 15.1 mg ml^{-1} isolated from a forest soil (Forbes) in the presence of 46.2 μmol ml^{-1} DFOB. C, Contour plot of two-dimensional ^{1}H NOESY of the sample from B. The corresponding off-diagonal cross-peak pattern for free DFOB, HS, and DFOB + HS is represented by thin dashed lines, thin solid lines and thick grey lines, respectively. These cross-peaks indicate regions of intra- and intermolecular associations via exchange and dipolar interactions of specific functional groups, as discussed in the text.

indicating that this marker was representative of DFOB and Cd^{II} association up to a 1 : 1 molar ratio, presumably representing DFOB·Cd. It also appears to indicate that the 4 h incubation time used throughout this study was sufficient for this interaction to develop. We cannot, on the basis of the data in Fig. 3(B) alone, rule out the possibility that this relationship was an analytical artifact, but note that the molar response levels off above the 1:1 ratio, as would be expected of Cd^{II} chelated to DFOB. In addition, the results from the experiments described below are consistent with this marker representing [DFOB·Cd]. The identity and formation mechanism of this *m/z* 140 marker are unknown, but a search of the NIH–NIST–EPA mass spectral library provided matches with alkyl-substituted pyrazolediones (results not shown), which were absent in thermolyzates of HS and DFOB, alone or together. The marker did not contain Cd because it lacked the characteristic isotope distribution pattern of Cd; it is probably a product of Cd-redirected bond scission and rearrangement pathway(s) of DFOB thermolysis.

[HS·Cd] marker

Fig. 3(C) shows the molar response of the *m/z* 57 peak (see Fig. 2) to Cd^{II} added to 1.25 μg μl^{-1} HS at pH 6.5; three replicate analyses are plotted (except at 10 mM Cd, just one analysis) to illustrate the raw variance. This marker could not be used above about 6 mM Cd (= 4.8 nmol Cd μg^{-1} HS) because the peak became too small to quantify. HS did not precipitate until > 32 nmol Cd μg^{-1} HS. The logarithmic regression fit through the data in Fig. 3(C) has $r^2 > 0.96$; this negative logarithmic relationship with the HS : Cd ratio is remniscient of a pH electrode response to [H_3O^+]. Within the scope of this study, we could not distinguish whether the *m/z* 57 marker had a non-linear analytical response to [HS·Cd], or whether the formation of the complex itself was a non-linear function of [Cd], in which case the marker may be responding linearly to [HS·Cd]. Certainly the latter is plausible, since HS would be expected to have a wide range of sites of different affinity, which would give rise to a non-linear dependence of complex formation on Cd concentration. The identity of this marker, based on a search of the NIH–NIST–EPA mass spectral library, yielded matches with trimethylpentenes, indicative of aliphatic residues in the HS.[22] The response mechanism may be related to the fact that Cd^{II} caused all HS thermolyzate peaks to decline, and yet this marker was more resistant than other peaks to the addition of Cd^{II}. This probably results from a lack of interaction of aliphatic domains with Cd-binding sites. The above uncertainties make the use of this marker problematic, but the advantage of the pyrolysis–GC–MS technique is that this marker, along with hundreds of others, is obtained with no additional analytical effort.

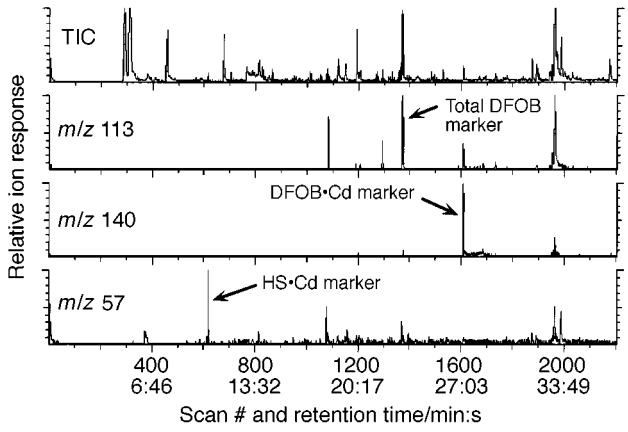

Fig. 2 Pyrolysis–GC–MS total ion chromatogram (TIC) and single-ion plots of *m/z* 113, 140, and 57 for a mixture of DFOB, Cd, and Chikugo HS, with arrows that point out the quantitative markers for total [DFOB], [DFOB·Cd], and [Cd·HS]. The marker for DFOB, detected using *m/z* 113, is an *N*-alkylpyrrolidinedione, probably formed from cyclization of the hydroxamate structure. The basis for the other two markers is discussed in the text.

*DFOB–HS–*Cd *relationships revealed by Pyrolysis–GC–MS*

The above three markers and their calibration curves were then employed for experiments to probe how DFOB association with HS (a fact already established from the NMR studies) interacts with Cd^{II}. Fig. 4 depicts results of mixing 5 mM each of DFOB and Cd^{II}, then adding various amounts of HS, followed by pyrolysis–GC–MS analysis. The black triangles show the total [DFOB] (via *m/z* 113 marker), which always corresponded to the expected value, hence there was no indication of DFOB degradation in any experiment. The [DFOB·Cd] (*via m/z* 140

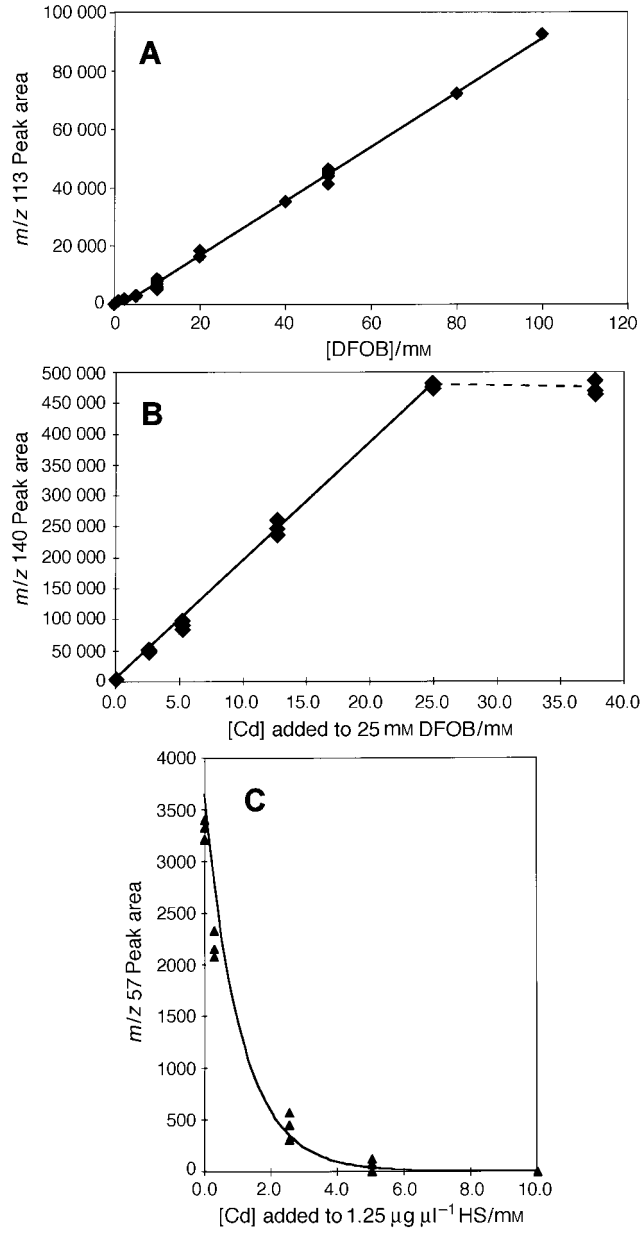

Fig. 3 Molar responses of DFOB, DFOB·Cd, and HS·Cd markers: A, plot of the peak area of *m/z* 113 versus [DFOB]; B, *m/z* 140 peak area *versus* 25 mM DFOB + Cd^{II}, and C, *m/z* 57 peak area *versus* 1.25 μg μl^{-1} HS + Cd^{II}.

marker, black squares) was near 5 mM at [HS] = 0, as expected, but declined with increasing [HS] until it was essentially zero at 1.25 μg HS μl^{-1} (shown by the arrow). The arrow in Fig. 4 indicates the [HS] used in all subsequent experiments.

An explanation for the result in Fig. 4 is that the HS simply out-competed DFOB for the Cd ions. However, this seems unlikely as DFOB is a very strong chelator of transition metals, (*e.g.* ref. 23) including Cd^{II}, (*e.g.* ref. 24) and also was allowed to incubate with Cd^{II} for 4 h before adding HS, which appeared to be sufficient time for DFOB·Cd formation [Fig. 3(B)]. In addition, based on the *m/z* 57 marker for HS·Cd, the ratio of Cd bound to HS was roughly constant, ranging from 1.8 to 1.3 nmol HS·Cd μg^{-1} HS for 0.25–2.5 μg μ^{-1} HS (data not shown). For example, at the point where [DFOB·Cd] decreases to zero (the arrow in Fig. 4), we estimate [HS·Cd] = 1.8 mM (expressed as mM of Cd bound to HS), leaving 3.2 mM Cd (out of 5 mM total) available for DFOB complexation. Therefore, it appears that Cd availability was not limiting the formation of DFOB·Cd.

An alternative explanation for the result in Fig. 4 is that DFOB was no longer available for chelating the Cd^{II} because it was interacting with HS; at the arrow in Fig. 4, all 5.0 mM of DFOB added is 'missing' or 'unavailable', because [DFOB·Cd] = 0 mM despite the 3.2 mM Cd available to complex with DFOB. It is also possible that all three were forming a ternary complex (*e.g.*, DFOB·Cd·HS). These alternative scenarios seem likely since we already know from the NMR experiments that DFOB·HS occurs extensively. However, to justify the presence of the ternary complex, it would require that the *m/z* 140 marker for DFOB·Cd is not formed from the DFOB·Cd·HS complex.

To test further whether HS was out-competing DFOB for Cd^{II}, we conducted a second experiment using the HS amount (1.25 μg HS μl^{-1}) that gave [DFOBCd] = 0 mM in the previous experiment (shown by the arrow in Fig. 4). We mixed into the HS solution various amounts of Cd^{II}, then added 5 mM DFOB. In effect, we changed the order in which reagents were added. Results of the DFOB·Cd analysis are shown in Fig. 5 (black squares), along with the '1 : 1' line which would be expected in the absence of HS [as in Figure 3(B)], or if DFOB was a far more powerful chelator than HS. At [Cd] ≤ 5 mM, the slope of [DFOB·Cd]/[Cd] is roughly parallel with the 1 : 1 line, indicating that DFOB chelated Cd^{II} away from HS. This is also evident from the [HS·Cd] data for experiments of [Cd] ≥ 5 mM, as follows: before the addition of DFOB, [HS·Cd] was about 5 mM, which dropped to 1.6 mM upon addition of DFOB (data not shown). Note that this [HS·Cd] value is similar to the 1.8 mM obtained in the previous experiment.

This value of [HS·Cd] = 1.6 mM can be subtracted from the 5–20 mM Cd^{II} added, leaving 3.4–18.4 mM Cd^{II} free to complex with the 5 mM DFOB in the system. This means that [Cd] was again not limiting the formation of DFOB·Cd in this experimental series. Instead, Fig. 5 shows that [DFOB·Cd] leveled off at 1.9 mM (indicated by the arrow), which means that [DFOB] was limiting, with apparently 1.9 mM available. Subtracting this value from the 5 mM DFOB that was added leaves 3.1 mM 'unavailable' DFOB, probably associated with HS.

The two experiments thus far ruled out any simple binary competition model, so the third experiment performed the remaining order of addition: various amounts of DFOB were first added to 1.25 μg HS μl^{-1}, then 5 mM Cd^{II} was mixed in last. Fig. 6 shows the results of the DFOB·Cd (black squares) and HS·Cd (open triangles) analyses, along with the same '1 : 1 line' from the previous figure. In the presence of DFOB, [HS·Cd] decreased to ≤ 0.4 mM, indicating free [Cd] ≥ 4.6 mM. Despite this available Cd^{II}, no DFOB·Cd was detected until [DFOB] was > 2.5 mM. Hence, once again, DFOB availability was the limiting factor for the formation of DFOB·Cd.

In the region of 5–20 mM added DFOB, the [DFOB·Cd]/[DFOB] slope did not parallel the 1 : 1 line (Fig. 6), suggesting that the situation was more complex than DFOB "saturating" HS sites, with the excess as free DFOB. Cadmium(II) is unlikely to be a factor in the less-than-unity slope since [Cd] that was free to form DFOB·Cd was constant (calculated from [HSCd] in Fig. 6). Currently, we hypothesize that the low-slope phenomenon is primarily due to a rapid exchange of DFOB with the surface of HS, as already shown by the NMR studies.

As a final point, the arrows in Figs. 4–6 point to solutions that can be directly compared, since they had the same final stoichiometry of 1.25 μg μl^{-1} HS, 5 mM DFOB and 5 mM Cd^{II}, but differed in the order of addition of reagents. To summarize, the Fig. 4 experiment (DFOB + Cd, then HS) yielded [DFOB·Cd] = 0.0 mM, leaving 5.0 mM DFOB unavailable; the

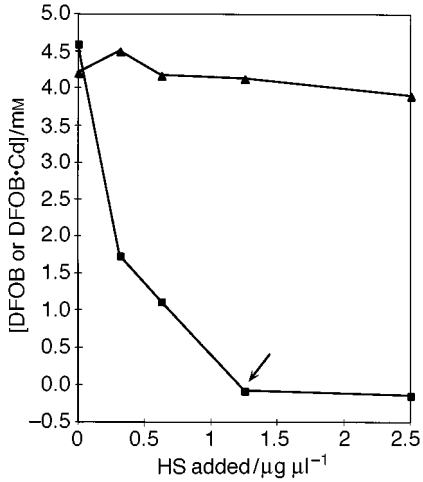

Fig. 4 Pyrolysis–GC–MS analysis of [DFOB·Cd] and total [DFOB] upon HS addition to DFOB·Cd. The black squares plot shows the result of varying amounts of HS added to a solution of 5 mM each DFOB and Cd^{II}. Starting with the expected ≈ 5 mM DFOB·Cd at zero [HS], as the HS concentration was increased, the DFOB·Cd marker shows a progressive decrease, reaching non-detectable levels at 1.25 μg HS μl^{-1} (arrow). This is also the [HS] used in subsequent figures. The arrow additionally points to the [DFOBCd] in a solution with the same stoichiometry as those indicated by arrows in Figs. 5 and 6. The black triangle plot shows total [DFOB], illustrating that this marker was independent of Cd^{II} or HS in the sample.

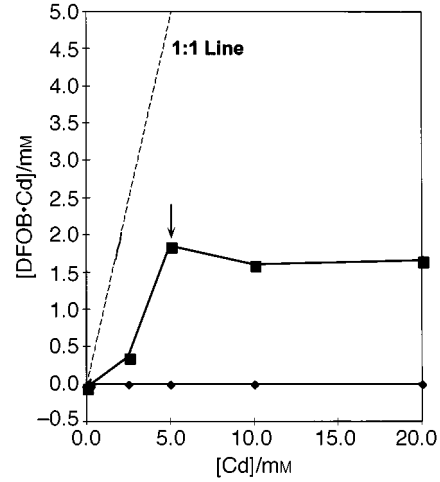

Fig. 5 Pyrolysis–GC–MS Analysis of [DFOB·Cd] upon DFOB addition to Cd·HS. Various amounts of Cd^{II} were added to HS, then 5 mM DFOB was added. [DFOB·Cd] at the end of the experiment are shown as black squares, along with the '1 : 1' line which would be expected in the absence of HS [as in Fig. 3(B)]. The plot of black diamonds shows [DFOB·Cd] prior to completing the experiment by addition of Cd^{II}, illustrating the lack of response of the 'blank' solutions. The arrow points to the [DFOB·Cd] in a solution with the same stoichiometry as those indicated by arrows in Figs. 4 and 6.

Fig. 5 experiment (HS + Cd, then DFOB) gave [DFOB·Cd] = 1.9 mM, leaving 3.1 mM DFOB unavailable; and the Fig. 6 experiment (HS + DFOB then Cd), exhibited [DFOBCd] = 0.4 mM, leaving 4.6 mM DFOB unavailable. In each case, [Cd] was not limiting. The explanation for these differences must await further studies of the complex associations revealed here, but it underscores the importance of the order of addition when experimenting with siderophores and HS. Also, because this is a system in which very high affinity complexes are formed, slow dissociation kinetics are possible, so that equilibrium may not have been reached during the course of the 8 h experiments. However, both issues of order of addition and non-equilibrium conditions are closer to the case of real systems such as the plant rhizosphere.

Conclusions

We applied 1-D and 2-D NMR techniques to obtain unprecedented kinetic and structural evidence of extensive DFOB association with HS in the absence of added metal ions. The use of Tiron in the extraction scheme greatly improved the quality of NMR spectra. However, the analytical advantage of the NMR is optimal at high analyte concentrations that may cause precipitation of HS by Cd^{II}. We therefore probed the interaction of this HS and DFOB association in the presence of Cd^{II}, using direct analysis of microliter volumes by pyrolysis–GC–MS. This technique yielded markers of total DFOB and apparent complexes of DFOB·Cd and HS·Cd. Although pyrolysis–GC–MS can be difficult or even treacherous to interpret alone owing to the formation of artifacts, (*e.g.* ref. 25) the relationships established by the NMR studies helped validate the use of the method in obtaining interactions of DFOB, HS and Cd^{II}. Unlike NMR, UV–visible spectrophotometry, ion-selective electrode and other metal–ligand measurements that are limited to non-paramagnetic and/or homogenous liquid-state studies, it is forseeable that the pyrolysis–GC–MS analysis can be extended to whole soils and sediments for the analysis of metal ion speciation.

The results consistently indicated that unavailable DFOB, in the form of DFOB·HS (or possibly DFOB·Cd·HS) led to significant decreases in the formation of the chelator complex, DFOB·Cd. In the stoichiometrically identical experiments (at arrows in Figs. 4-6), more than half of the added DFOB was unavailable for chelating Cd^{II}. Although the DFOB·HS complex appeared to be weak, the rapid exchange may be an important mechanism for the observed decrease in [DFOB·Cd]. We could not discount the possibility of a sub-population of strong DFOB·HS complex as a contributing mechanism. The results do not fit the pattern of simple competitive equilibria, owing to the strong dependence of results on the order of addition of reagents. The results of this study indicate that the basis of existing metal ion speciation models—competition among ions for HS ligand sites, (*e.g.* ref. 26) and distribution of the metal ion among different ligands (*e.g.*, ref. 13, 17)—is incomplete and should incorporate the possibility of interaction and its kinetics between the soluble ligands and HS. However, as there appears to be only one other report of HS–ligand association,[16] it will be some time before a database sufficient for use in models can be established.

In any given study, the reaction conditions and the chemical nature of the isolated HS can vary, but it is clear such organic ligand–HS interactions do occur and can significantly alter the chemistry, and hence potentially the bioavailability, of metal ions. In this study, the bioavailability issue is particularly relevant since the organic ligand studied, DFOB, represents a major class of chemical synthesized by bacteria to acquire metal ions, while HS is nearly ubiquitous in soil and sediment. Therefore, understanding the bioavailability of transition metal ions in real systems such as the rhizosphere is bound to depend on the biogenic ligand chemistry, poorly understood HS structures and now the interactions of HS with biogenic ligands.

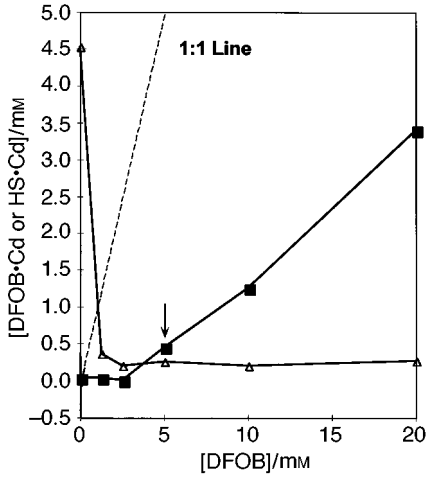

Fig. 6 Pyrolysis–GC–MS Analysis of [DFOB·Cd] and [HS·Cd] upon Cd^{I} addition to DFOB·HS. Various amounts of DFOB were first added to 1.25 μg HS μl^{-1}, then 5 mM Cd^{II} was mixed in. Results of [DFOB·Cd] (black squares) and [HS·Cd] (open triangles) analyses are shown along with the same '1 : 1 line' as in Fig. 5. The arrow points to the [DFOB·Cd] in a solution with the same stoichiometry as those indicated by arrows in Figs. 4 and 5.

This study was supported, in part, by the USEPA funded (grant No. R819658) Center for Ecological Health Research at the University of California–Davis, USEPA grant No. R825960010 and US Department of Energy grant No. DE-FG07-96ER20255. We acknowledge the UK Medical Research Council Biomedical NMR Centre for use of NMR instrumentation and thank Kevin Armbrust of DuPont Agricultural Products for the rice soils.

References

1 *Iron Chelation in Plants and Soil Microorganisms*, ed. Barton, L. L,. and Hemming, B. C., Academic Press, San Diego, 1993, and references cited therein.
2 Fan, T. W.-M., Lane, A. N., Pedler, J., Crowley, D., and Higashi, R. M., *Anal. Biochem.*, 1997, **251**, 57.
3 Buffle, J., *Complexation Reactions in Aquatic Systems: an Analytical Approach*, Ellis Horwood, Chichester, 1988.
4 Hayes, M. H. B., in *Advances in Soil Organic Matter Research: the Impact on Agriculture and the Environment*, ed. Wilson, W.S., The Royal Society of Chemistry, Cambridge, 1991, p. 3.
5 Grimm, D. M., Azarraga, L. V., Carrelra, L. A., Susetyo, W., *Environ. Sci. Technol.*, 1991, **25**, 1427.
6 Petronio, B. M., Cosma, B., Mazzucotelli, A., and Rivaro, P., *Intern. J. Environ. Anal. Chem.*, 1993, **54**, 45.
7 Westall, J. C., Jones, J. D., Turner, G. D., Zachara, J. M., *Environ. Sci. Technol.*, 1995, **29**, 951.
8 Benedetti, M. F., Milne, C. J., Kinniburgh, D. G., van Riemsdijk, W. H., and Koopal, L. K., *Environ. Sci. Technol.*, 1995, **29**, 446.
9 Kinniburgh, D. G., Milne, C. J., Benedetti, M. F., Pinheiro, J. P., Filius, J., Koopal, L. K., van Riemsdijk, W. H., *Environ. Sci. Technol.*, 1996, **30**, 1687.
10 Jin, X., Bailey, G. W. ,Yu, Y. S., and Lynch, A. T., *Soil Sci.*, 1996, **161**, 509.
11 Senesi, N., Sposito, G., Bradford, G. R., and Holtzclaw, K. M., *Water Air Soil Pollut.*, 1991, **55**, 409.
12 Hernandez, T., Moreno, J. I., and Costa, F., *Agrochimica*, 1993, **37**, 12.
13 Allison, J. D., and Perdue, E. M., in *Humic Substances in the Global Environment and Implications on Human Health*, ed. Senesi, N., and Miano, T. M., Elsevier, Amsterdam, 1994, pp. 927–942.

14 Glaus, M. A., Hummel, W., and van Loon, L. R., *Environ. Sci. Technol.*, 1995, **29**, 2150.
15 Powell, P. E., Szaniszlo, P. J., Cline, G. R., and Reid, C. P. P., *J. Plant Nutr.*, 1982, **5**, 653.
16 Solinas, V., in *Humic Substances in the Global Environment and Implications on Human Health*, ed. Senesi, N., and Miano, T. M., Elsevier, Amsterdam, 1994, p. 1183.
17 Hancock, R. D., and Martell, A. E., *Chem. Rev.*, 1989, **89**, 1875.
18 Olk, D. C., Cassman, K. G., and Fan, T. W.-M., *Geoderma*, 1995, **65**, 195.
19 Davies, G., Fataftah, A., Cherkasskiy, A., Radwan, A., Jansen, S. A., Paciolla, M., and Ghabbour, E. A., paper presented at the 8th International Humic Substances Society Meeting, 1994.
20 Lane, A. N., Bauer, C. J., and Frenkiel, T. A., *Eur J. Biophys.*, 1993, **21**, 425.
21 Borgias, B., Hugi, A. D., and Raymond, K. N., *Inorg. Chem.*, 1989, **28**, 3538.
22 Bracewell, J. M., Haider, K., Larter, S. R., and Schulten, H.-R., *in Humic Substances II: in Search of Structure*, ed. Hayes, M. H. B., MacCarthy, P., Malcolm, R. L., and Swift, R. S., Wiley, Chichester, 1989, pp. 182–222.
23 Anderegg, G., L'Eplattenier, F., and Schwarzenbach, G., *Helv. Chim. Acta*, 1963, **46**, 1400.
24 Evers, A., Hancock, R. D., Martell, A. E., and Motekaitis, R. J., *Inorg. Chem.*, 1989, **28**, 2189.
25 Nip, M., de Leeuw, J. W., Holloway, P. J., Jensen, J. P. T., Sprenkels, J. C. M., de Pooter, M., and Sleeckx, J. J. M., *J. Anal. Pyrol.*, 1987, **11**, 287.
26 Tipping, E., *Environ. Sci. Technol.*, 1993, **27**, 520.

Paper 7/08177D
Received November 13, 1997
Accepted March 24, 1998